QUASISTATIONARY ELECTRON STATES AND THE CONDUCTIVITY OF A SYMMETRIC THREE-BARRIER RESONANT TUNNEL STRUCTURE

M.V. TKACH, YU.O. SETI

Chernivtsi National University
(2, Kotsyubynskyi Str., Chernivtsi 58012, Ukraine; e-mail: ktf@chnu.edu.ua)

PACS 73.21.Fg, 72.30.+q, 73.63.Hs, 73.90.+f

The evolution of spectral parameters (resonance energies and widths) of quasistationary electron states and its dependence on geometrical parameters of a nanosystem have been studied in the framework of the rectangular and δ-like potential barrier models for a symmetric three-barrier resonant tunnel structure (TBRTS). The conductivity of symmetric TBRTS has been determined in the low-electric-field approximation. The maximal magnitudes of conductivity in the model of δ-like potential barriers were found to be ten times as low as that in a more realistic model of rectangular potentials, due to the neglect of the difference between electron effective masses in the wells and barriers.

1. Introduction

Three-barrier plane nanostructures draw attention of researchers from both fundamental and application's viewpoints. Interest to studying the quasistationary electron states (QSESs) in such TBRTSs has considerably grown after finding that those nanosystems can be a base element for an experimentally created quantum cascade laser [1, 2] which operates in the terahertz frequency range, urgent for applications.

Theoretical works [3–6] aimed at studying the properties of QSES spectroscopic parameters – resonance energies (REs) and resonance widths (RWs) – in resonant tunnel structures (RTSs), as well as the conductivity of the system, when an electron beam travels through it, have been known for more than ten years. However, there is no satisfactory coincidence between theoretical and experimental results till now.

The main reason of theoretical complications is the circumstance that, while studying the conductivity properties in RTSs, it is necessary to solve the complete Schrödinger equation that describes the interaction between electrons and an electromagnetic field in an open system. The solution of such a problem appears rather difficult even for the simple model of effective masses and δ-like potential barriers which is often used in many works [7–12]. Even a simple task of calculating the QSES spectroscopic parameter s for an RTS with weak potential barriers, for which a solution of the stationary Schrödinger equation is needed, is also faced with the known difficulties typical of the theory of scattering in open low-dimensional nanosystems.

Some important features in the behavior of the transmission factor and QSES spectral parameters for symmetric TBRTSs were shown in works [13, 14]. In work [13], the phenomenon of resonance energy collapse for QSES pairs at an increase of the interior potential barrier strength above the total strength of external barriers in a symmetric TBRTS was discovered and carefully examined in the framework of the δ-like potential model. In the same work, the origin of collapse was found: it is an analog of a phase transition of the second kind with respect to the asymmetry parameter that characterizes the relative difference between the probabilities to find electrons in either of two nanosystem wells.

In work [14], the collapse phenomenon for electron resonance pairs was analyzed in a more realistic model of rectangular potentials with regard for the difference between effective masses of a electron in the wells and the barriers of symmetric TBRTS. It was shown that, though the δ-barrier model describes the dependences of QSES spectral parameters on the interior barrier strength (thickness) correctly at the qualitative level, but the whole picture is shifted toward the short-wave spectral range with respect to the results of the rectangular potential model, with the resonance width of every QSES being several times overestimated.

In theoretical works [7–12], either the RTS conductivity or the reduced currents obtained at the passage of electrons that interact with an electromagnetic field through the RTS was calculated in the framework of the δ-like barrier model. The results obtained demonstrate that the physical quantities under investigation are sensitive to the resonance widths of those QSESs which are engaged into quantum-mechanical transitions.

In this work, the conductivity of symmetric TBRTS was studied in the framework of the rectangular potential barrier model for a nanosystem with $In_{0.53}Ga_{0.47}As$ wells and $In_{0.52}Al_{0.48}As$ barriers as an example. The model of rectangular potentials, which is more realistic than the δ-barrier one, was shown to increase the maximal values of TBRTS conductivity by a factor of several tens.

2. Conductivity of Symmetric TBRTS in the Rectangular and δ-Like Potential Barrier Models

An open symmetric TBRTS is considered in a Cartesian coordinate system. The geometrical parameters of the system are illustrated in Fig. 1. An insignificant difference between the lattice constants in the layers-wells, $a_0 = 0.5868$ nm (media 0, 2, 4, and 6 in Fig. 1,*a*), and layers-barriers, $a_1 = 0.5867$ nm (media 1, 3, and 5), of RTSs allows the nanosystem to be studied in the framework of the models of effective masses and rectangular potential barriers (Fig. 1,*b*):

$$m(z) = \begin{cases} m_0, \\ m_1, \end{cases} \qquad U(z) = \begin{cases} 0, & \text{reg. } 0,\ 2,\ 4,\ 6, \\ U, & \text{reg. } 1,\ 3,\ 5, \end{cases} \tag{1}$$

where b is the width of each well, Δ_1 is the width of external barriers, and Δ is the interior barrier width.

Let an electron with the charge $-e$ and the energy E, which moves perpendicularly to the TBRTS planes, fall onto the structure from the left. The RTS conductivity is determined by the current density through the nanosystem, which is determined, according to quantum mechanics, by the wave function of the electron that interacts with a time-periodic electromagnetic field. The wave function $\Psi(z,t)$ satisfies the complete Schrödinger equation

$$i\hbar\frac{\partial\Psi(z,t)}{\partial t} = (H + H(z,t))\,\Psi(z,t), \tag{2}$$

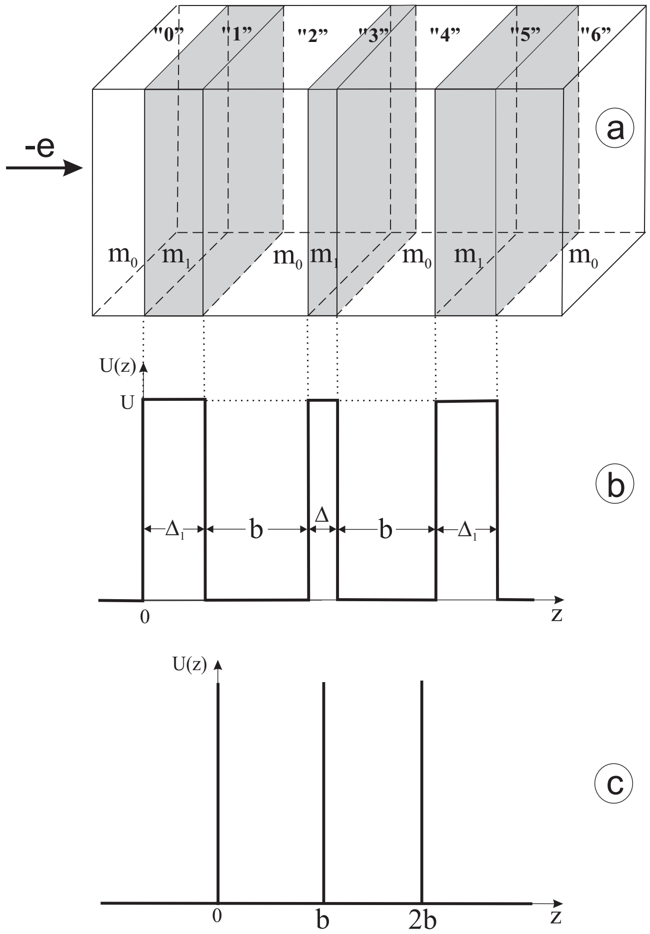

Fig. 1. Geometrical (*a*) and energy (*b* and *c*) schemes of symmetric TBRTS in the rectangular (*b*) and δ-like (*c*) potential models

where

$$H = -\frac{\hbar^2}{2}\frac{\partial}{\partial z}\frac{1}{m(z)}\frac{\partial}{\partial z} + U(z) \tag{3}$$

is the electron Hamiltonian of the stationary problem, and

$$H(z,t) = -e\epsilon\big(z\,\theta(z) + (2b + 2\Delta_1 + \Delta - z)\times$$

$$\times\theta(z - 2b - 2\Delta_1 - \Delta)\big)\big(e^{i\omega t} + e^{-i\omega t}\big) \tag{4}$$

is the Hamiltonian of interaction between the electron and a time-varying electromagnetic field with the frequency ω and the strength amplitude ϵ.

The solution of Eq. (2) is sought in the weak signal approximation [7–12], in the form

$$\Psi(z,t) = \Psi_0(z)\,e^{-i\omega_0 t} + \Psi_1(z,t)\,, (\omega_0 = E/\hbar), \tag{5}$$

where the function $\Psi_0(z)$ is a solution of the stationary Schrödinger equation

$$H\,\Psi_0(z) = E\,\Psi_0(z). \quad (6)$$

The first-order correction is sought in the single-mode approximation in the form

$$\Psi_1(z,t) = \Psi_{+1}(z)\, e^{-i(\omega_0+\omega)t} + \Psi_{-1}(z)\, e^{-i(\omega_0-\omega)t}. \quad (7)$$

Keeping the terms of the first order of smallness and taking Eqs. (2), (5), and (6) into account, the following equations for both components $\Psi_{\pm 1}(z,t)$ of the function $\Psi_1(z,t)$ are obtained:

$$\left(-\frac{\hbar^2}{2}\frac{\partial}{\partial z}\frac{1}{m(z)}\frac{\partial}{\partial z} + U(z) - \hbar(\omega_0 \pm \omega)\right)\Psi_{\pm 1}(z) +$$

$$+H(z)\,\Psi_0(z) = 0. \quad (8)$$

Here,

$$H(z) = -e\epsilon\big(z\,\theta(z) + (2b + 2\Delta_1 + \Delta - z)\times$$

$$\times\theta(z - 2b - 2\Delta_1 - \Delta)\big).$$

The solution of the stationary Schrödinger problem (6) is tried in the form

$$\Psi_0(z) = \Psi_0^{(0)}(z)\theta(-z) + \Psi_0^{(6)}(z)\theta(z - z_5) +$$

$$+\sum_{p=1}^{5}\Psi_0^{(p)}(z)\left[\theta(z - z_{p-1}) - \theta(z - z_p)\right] =$$

$$= \left(e^{ik^{(0)}z} + B^{(0)}e^{-ik^{(0)}z}\right)\,\theta(-z) +$$

$$+A^{(6)}e^{ik^{(6)}z}\theta(z - z_5) +$$

$$+\sum_{p=1}^{5}\left(A^{(p)}e^{ik^{(p)}(z - z_{p-1})} + B^{(p)}e^{-ik^{(p)}(z - z_{p-1})}\right)\times$$

$$\times\left[\theta(z - z_{p-1}) - \theta(z - z_p)\right]. \quad (9)$$

Here,

$$k^{(0)} = k^{(2)} = k^{(4)} = k^{(6)} = k = \hbar^{-1}\sqrt{2m_0E};$$

$$k^{(1)} = k^{(3)} = k^{(5)} = -\hbar^{-1}\sqrt{2m_1(E - U)};$$

$$z_0 = 0;\ z_1 = \Delta_1;\ z_2 = b + \Delta_1;\ z_3 = b + \Delta_1 + \Delta;$$

$$z_4 = 2b + \Delta_1 + \Delta;\ z_5 = 2(b + \Delta_1) + \Delta.$$

The unknown coefficients $B^{(0)}, A^{(6)}$, $A^{(p)}$, and $B^{(p)} (p = 1\ldots 5)$ are determined from the matching conditions for the wave functions and their density fluxes at each nanosystem interface,

$$\begin{cases} \Psi_0^{(i)}(z_i) = \Psi_0^{(i+1)}(z_i); \quad (i = 0,\ \ldots,\ 5) \\ \frac{1}{m_{0(1)}}\left.\frac{d\Psi_0^{(i)}}{dz}\right|_{z=z_i} = \frac{1}{m_{1(0)}}\left.\frac{d\Psi_0^{(i+1)}(z)}{dz}\right|_{z=z_i}, \end{cases} \quad (10)$$

with regard for the normalization condition

$$\int_{-\infty}^{\infty}\Psi_0^*(k'z)\Psi_0(kz)\,dz = \delta(k - k'). \quad (11)$$

The solutions of the inhomogeneous equations (8) are superpositions of the functions

$$\Psi_{\pm 1}(z) = \Psi_{\pm}(z) + \Phi_{\pm}(z), \quad (12)$$

where $\Psi_{\pm}(z)$ are the solutions of homogeneous Eq. (8), and $\Phi_{\pm}(z)$ are the partial solutions of nonhomogeneous Eq. (8).

The solutions of the homogeneous equations (8) are tried in the form

$$\Psi_{\pm}(z) = \Psi_{\pm}^{(0)}(z)\theta(-z) + \Psi_{\pm}^{(6)}(z)\theta(z - z_5) +$$

$$+\sum_{p=1}^{5}\Psi_{\pm}^{(p)}(z)\left[\theta(z - z_{p-1}) - \theta(z - z_p)\right] =$$

$$= B_{\pm}^{(0)}e^{-ik_{\pm}^{(0)}z}\theta(-z) + A_{\pm}^{(6)}e^{ik_{\pm}^{(6)}(z - z_5)}\theta(z - z_5) +$$

$$+\sum_{p=1}^{5}\left(B_{\pm}^{(p)}e^{-ik_{\pm}^{(p)}(z - z_{p-1})} + A_{\pm}^{(p)}e^{ik_{\pm}^{(p)}(z - z_{p-1})}\right)\times$$

$$\times\left[\theta(z - z_{p-1}) - \theta(z - z_p)\right], \quad (13)$$

where

$$k_{\pm}^{(0)} = k_{\pm}^{(2)} = k_{\pm}^{(4)} = k_{\pm}^{(6)} = k_{\pm} = \hbar^{-1}\sqrt{2m_0(E \pm \hbar\omega)};$$

$$k_{\pm}^{(1)} = k_{\pm}^{(3)} = k_{\pm}^{(5)} = \hbar^{-1}\sqrt{2m_1\left((U-E)\mp\hbar\omega\right)}\,. \tag{14}$$

The exact partial solutions of Eqs. (8) are known:

$$\Phi_{\pm}(z) = \sum_{p=1}^{5}\left(\mp\frac{e\epsilon}{\hbar\omega}z\,\Psi_0^{(p)}(z) + \frac{e\epsilon}{m_p\omega^2}\frac{d\Psi_0^{(p)}(z)}{dz}\right)\times$$

$$\times\left[\theta(z-z_{p-1})-\theta(z-z_p)\right]\mp\frac{e\epsilon}{\hbar\omega}z_5\Psi_0^{(6)}(z_5)\,\theta(z-z_5). \tag{15}$$

Therefore, the general solution of Eqs. (8) can be represented in the form

$$\Psi_{\pm 1}(z) = \Psi_{\pm 1}^{(0)}(z)\,\theta(-z) + \Psi_{\pm 1}^{(6)}(z)\,\theta(z-z_5) +$$

$$+\sum_{p=1}^{5}\Psi_{\pm 1}^{(p)}(z)\ \left[\theta(z-z_{p-1})-\theta(z-z_p)\right]. \tag{16}$$

The continuity conditions for the wave function (16) and the corresponding fluxes at the nanosystem interfaces,

$$\begin{cases} \Psi_{\pm 1}^{(i)}(z_i) = \Psi_{\pm 1}^{(i+1)}(z_i)\,; \qquad (i=0,...,5) \\ \left.\frac{d\,\Psi_{\pm 1}^{(i)}(z)}{m_{0(1)}dz}\right|_{z=z_i} = \left.\frac{d\,\Psi_{\pm 1}^{(i+1)}(z)}{m_{1(0)}dz}\right|_{z=z_i}\,; \end{cases} \tag{17}$$

give rise to a system of 12 inhomogeneous equations which are used to determine all 12 unknown coefficients $B_{\pm}^{(0)}$, $A_{\pm}^{(6)}$, $B_{\pm}^{(p)}$, and $A_{\pm}^{(p)}$ $(p = 0,\ldots,5)$. Hence, the functions $\Psi_{\pm}(z)$ and the first-order correction $\Psi_1(z,t)$ are found unambiguously now, so that the complete wave function $\Psi(z,t)$ is also known.

According to quantum mechanics, the current density created by noninteracting electrons with the concentration n_0 is determined by the formula

$$j(z,t) =$$

$$= \frac{e\hbar_0}{2m(z)}\left(\Psi(z,t)\frac{\partial}{\partial z}\Psi^*(z,t) - \Psi^*(z,t)\frac{\partial}{\partial z}\Psi(z,t)\right). \tag{18}$$

Since the TBRTS dimensions are small in comparison with the electromagnetic wavelength, we use the quasiclassical approximation to calculate the reduced current density which governs [10–12] the real part of the nanosystem conductivity:

$$\sigma(\omega) = \frac{\hbar^2\omega\ n_0}{2z_5 m_0\epsilon^2}\times$$

$$\times\left[k_+\left(\left|B_+^{(0)}\right|^2 + \left|A_+^{(6)}\right|^2\right) - k_-\left(\left|B_-^{(0)}\right|^2 + \left|A_-^{(6)}\right|^2\right)\right]. \tag{19}$$

This technique was used to calculate the conductivity $\sigma^{\delta}(\omega)$ of TBRTS in the framework of the models of effective masses and δ-like potential barriers (Fig. 1,*c*),

$$m_{\delta}(z) = m_0;$$

$$U_{\delta}(z) = U\left(\Delta_1\left(\delta(z)+\delta(z-2b)\right)+\Delta\delta(z-b)\right), \tag{20}$$

with the Hamiltonians

$$H_{\delta} = -\frac{\hbar^2}{2m_0}\frac{\partial^2}{\partial z^2}+$$

$$+U\left(\Delta_1\delta(z)+\Delta\delta(z-b)+\Delta_1\delta(z-2b)\right), \tag{21}$$

$$[c]lH_{\delta}(z,t) = -e\epsilon\left(z\,\theta(z)+(2b-z)\ \theta(z-2b)\right)\times$$

$$\times\left(e^{i\omega t}+e^{-i\omega t}\right). \tag{22}$$

Since the analytical calculation of the conductivity $\sigma^{\delta}(\omega)$ in this model is similar to that for a TBRTS with rectangular potentials, being at the same time much simpler, it is not presented here.

The analysis of QSES spectral parameters and the conductivity calculated in the framework of both models was carried out, taking a symmetric TBRTS consisting of $In_{0.53}Ga_{0.47}As$ potential wells and $In_{0.52}Al_{0.48}As$ potential barriers as an example. This TBRTS was intensively studied in experimental works [15, 16].

3. Discussion of the Results Obtained

The peculiarities of the conductivity $\sigma(\omega)$ behavior and their dependences on the TBRTS geometrical parameters are expedient to be studied with regard for the dependences of electron resonance energies and widths on the thickness Δ of the interior barrier in the nanosystem.

In Fig. 2, the dependences of the resonance widths $\Gamma_{n\ell(u)}$ and the energies $E_{n\ell(u)}$ for first three QSES pairs in a symmetric TBRTS on the interior barrier thickness Δ calculated in both models of potential are depicted. Here, the subscripts ℓ and u correspond to the lower and upper states, respectively. The geometrical parameters of TBRTS are $b = 15a_0$ and $\Delta_1 = 4a_0$. The figure also

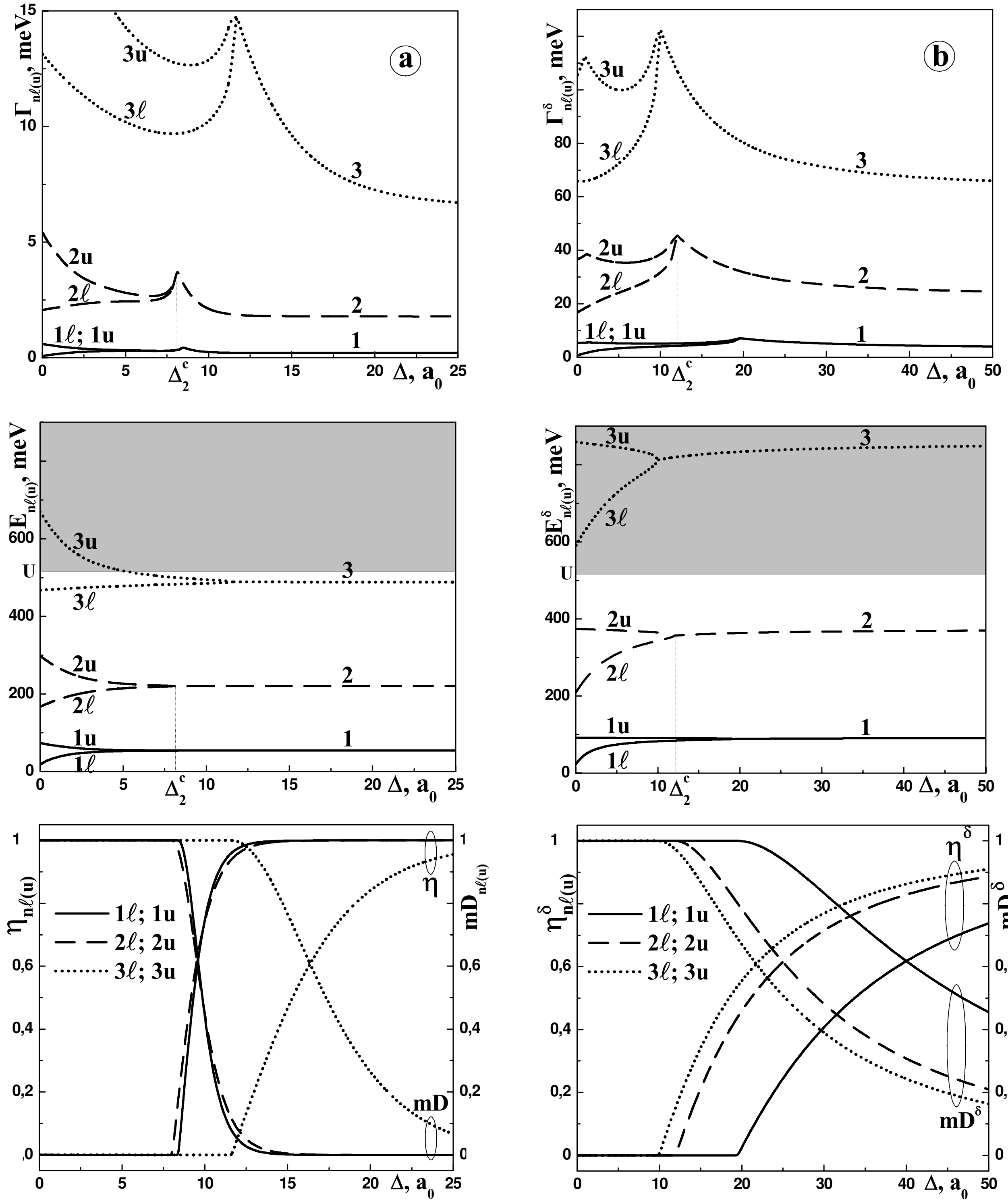

Fig. 2. Dependences of $\Gamma_{n\ell(u)}$, $E_{n\ell(u)}$, $\eta_{n\ell(u)}$, and $mD_{n\ell(u)}$ on the interior barrier thickness Δ in the rectangular (a) and δ-like (b) potential barrier models at $b = 15a_0$ and $\Delta_1 = 4a_0$

exhibits the Δ-dependences of the maximum of transmission factors $mD_{n\ell(u)}$ and the asymmetry ratios

$$\eta_{n\ell(u)} = \left| \frac{P^{(1)}_{n\ell(u)} - P^{(2)}_{n\ell(u)}}{P^{(1)}_{n\ell(u)} + P^{(2)}_{n\ell(u)}} \right|,$$

where

$$P^{(1,2)}_{n\ell(u)} = \int\limits_{(z_1,z_3)}^{(z_2,z_4)} \left| \Psi^{(1,2)}_{n\ell(u)}(z) \right|^2 dz,$$

which characterizes the relative difference between the probabilities $P_{n\ell(u)}$ for an electron to be found in the corresponding states $|n\ell(u)\rangle$ in the first (left, superscript (1)) and the second (superscript (2)) potential well. Those quantities are similar to the parameters of a phase transition of the second kind.

It is evident from the figure that the collapse scenarios for the spectral parameters (resonance energies and widths), as well as for the asymmetry ratios $\eta_{n\ell(u)}$ and the transmission factors $mD_{n\ell(u)}$, are qualitatively identical in both potential models. The quantitative difference consists in that the $E^{\delta}_{n\ell(u)}$ values are larger than the $E_{n\ell(u)}$ ones by tens of percents for the same interior barrier thickness, whereas $\Gamma^{\delta}_{n\ell(u)}$ are several times larger than $\Gamma_{n\ell(u)}$ in this case. In every n-th QSES pair, the collapse of spectral parameters occurs at those critical values Δ^c_n of interior barrier thickness, at which $\eta_{n\ell(u)}$ drastically grows to 1, and $mD_{n\ell(u)}$ drastically vanishes.

In the δ-barrier model, the critical values of interior barrier thickness, at which the resonance energies and widths collapse, are shifted toward larger magnitudes with respect to those obtained in the rectangular model.

Hence, the whole interval of interior barrier widths ($0 \le \Delta \le \infty$) can be divided into the "pre-collapse" ($\Delta < \Delta^c_n$) and "post-collapse" ($\Delta \ge \Delta^c_n$) regions for every n-th QSES pair.

Now, we can analyze the dependence of the conductivity $\sigma(\omega)$ on the interior barrier thickness Δ in a symmetric TBRTS and the injection current density; the latter, in the case of a flux of monoenergetic electrons with the concentration n_0, is unambiguously determined in terms of the electron energy E.

In Fig. 3,*a*, the results of calculations of $\sigma(\omega)$-dependence in the framework of rectangular barrier model for various interior barrier thicknesses $\Delta = 0$, 2, 4, 6, 8, 10, and $12a_0$ are presented. The TBRTS parameters are $b = 15a_0$ and $\Delta_1 = 4a_0$. The concentration of electrons incident on the RTS is $n_0 = 10^{16}$ cm^{-3}. Their energy is assumed to coincide with the resonance energy of the upper quasistationary state of the first resonance pair ($E = E_{1u}$).

In Fig. 3,*b*, the dependences of the resonance electron energies $E_{n\ell}$, E_{nu}, and E_n on the interior barrier thickness Δ are shown. Here, the arrows indicate the quantum-mechanical transitions between those QSESs which are associated with peaks (negative or positive) in the conductivity $\sigma(\omega)$. The results of analogous calculations in the framework of the δ-barrier model are exhibited in Figs. 3,*c* and *d*.

Figure 3 testifies that the rectangular barrier (Figs. 3,*a* and *b*) and δ-barrier (Figs. 3 *b* and *c*) models produce qualitatively similar results, although the whole picture becomes shifted in the latter case toward the higher energy range, and the maxima of $\left|\sigma^{\delta}(\omega)\right|$ turn out to be underestimated by a factor of 20 to 50. This situation results from the fact that the δ-barrier model does not take the difference between the effective masses in wells and barriers into account, which gives rise to a manifold increase of the resonance widths of all QSESs [14]. Since all max $|\sigma(\omega)|$-values are reciprocal to the product of the resonance widths of both QSESs, between which the transition occurs, the max $\left|\sigma^{\delta}(\omega)\right|$-heights turn out to be underestimated by a factor of several tens with respect to their max $|\sigma(\omega)|$-counterparts in the rectangular barrier model.

The dependences of $\sigma(\omega)$ on geometrical TBRTS parameters are qualitatively identical in both potential models, irrespective of the incident electron energy. Therefore, the subsequent analysis of conductivity properties will be carried out in the framework of the rectangular potential model only.

From Figs. 3,*a* and *b*, one can see that, if the energy of electrons incident on TBRTS coincides with the resonance energy of the upper state of the first QSES pair ($E = E_{1u}$), the quantum transition $1u \to 1\ell$ is accompanied by the emission of an electromagnetic wave, so that a negative conductivity is observed in the low-frequency spectral range. At the same time, a positive conductivity is observed in the high-frequency range of the spectrum owing to the transition $1u \to 2\ell$ with the absorption of an electromagnetic wave.

As the thickness Δ grows, the position of the minimum in the negative conductivity $\sigma(\omega)$ shifts to the region of low frequencies ω or low energies $\hbar\omega = E_{1u} - E_{1\ell}$, and its absolute value vanishes. The origin of such an evolution can be understood from Fig. 3,*b*. Really, when Δ increases, the distance between the resonance energies E_{1u} and $E_{1\ell}$ tends to zero. Therefore, the frequency of the transition $1u \to 1\ell$ and its intensity decrease, and, respectively, the quantity $|\min \sigma(\omega)|$ vanishes. After the

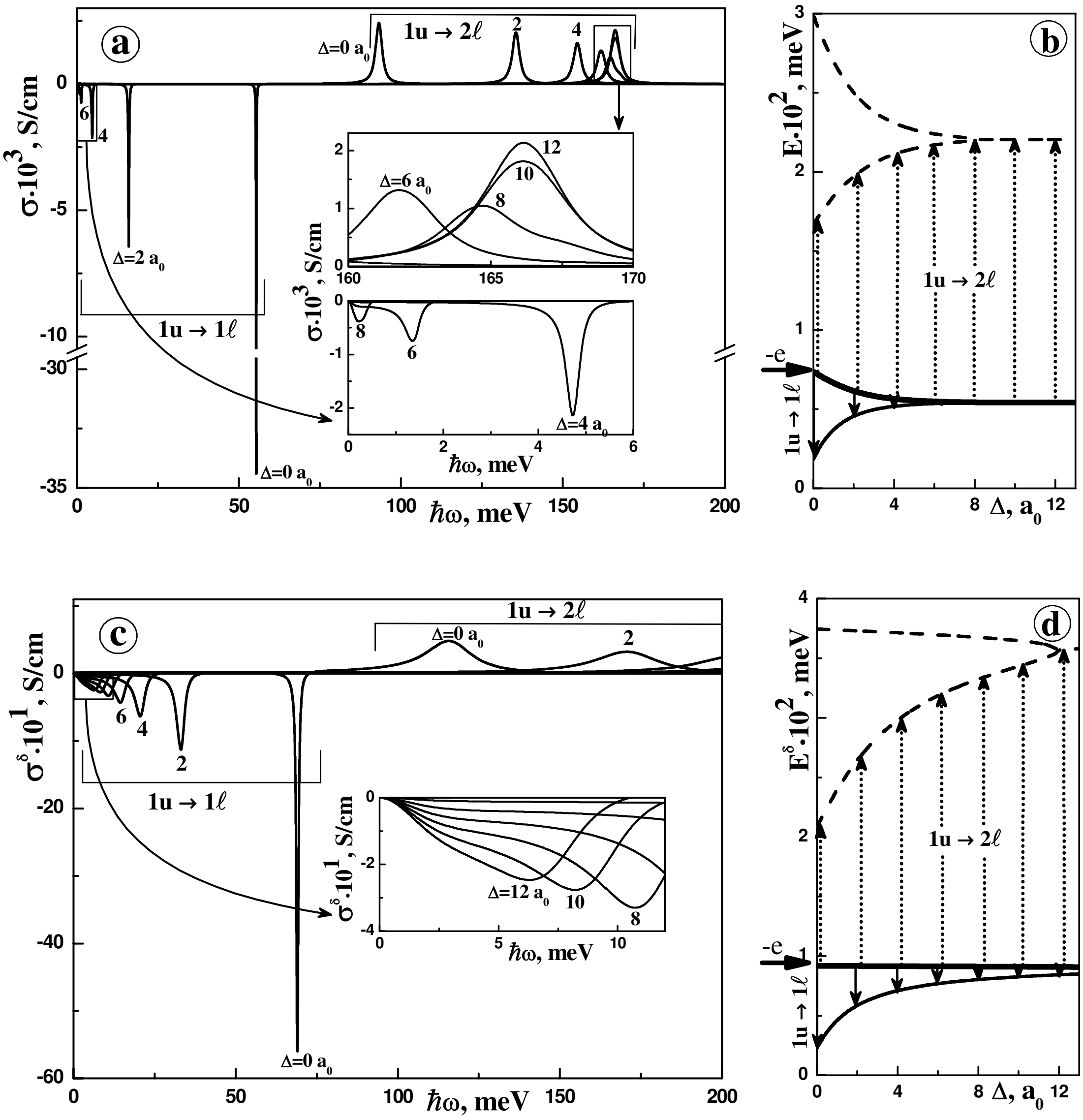

Fig. 3. Dependences of conductivity σ on the field energy $\hbar\omega$ (at the energy $E = E_{1\ell}$ and the concentration $n_0 = 10^{16}$ cm^{-3} of incident electrons) and the resonance electron energies E on the interior barrier thickness Δ in the rectangular (a and b) and δ-like (c and d) potential models at $b = 15a_0$ and $\Delta_1 = 4a_0$

first QSES pair collapses, i.e. after the degeneration of those states into a single state ($n = 1$), the transitions $1u \to 1\ell$ do not exist any more.

The positive peak of the conductivity is formed by the quantum transition $1u \to 2\ell$ (Fig. 3,a). Therefore, as is seen from the figure, the growth of Δ is accompanied by the peak shift toward the higher-frequency range ($\hbar\omega = E_{2\ell} - E_{1u}$). After the collapse, the energy of transitions corresponds to the difference between the resonance energies of the second and the first collapsed pair of QSESs ($\hbar\omega = E_2 - E_1$). The intensity of the positive conductivity peak decreases, if Δ increases in the pre-collapse region, and saturates in the post-collapse one. Such an evolution of $\sigma(\omega)$ is explained by the fact that the probability density of finding an electron in the TBRTS potential wells (the first and the second one) becomes redistributed, as the interior barrier thickness Δ increases.

In Fig. 4, the evolution of the conductivity $\sigma(\omega)$ with a change of the interior barrier thickness Δ is depicted for various energies of electrons incident on TBRTS ($E = E_{2\ell}$, E_{2u}, $E_{3\ell}$). The calculations were carried

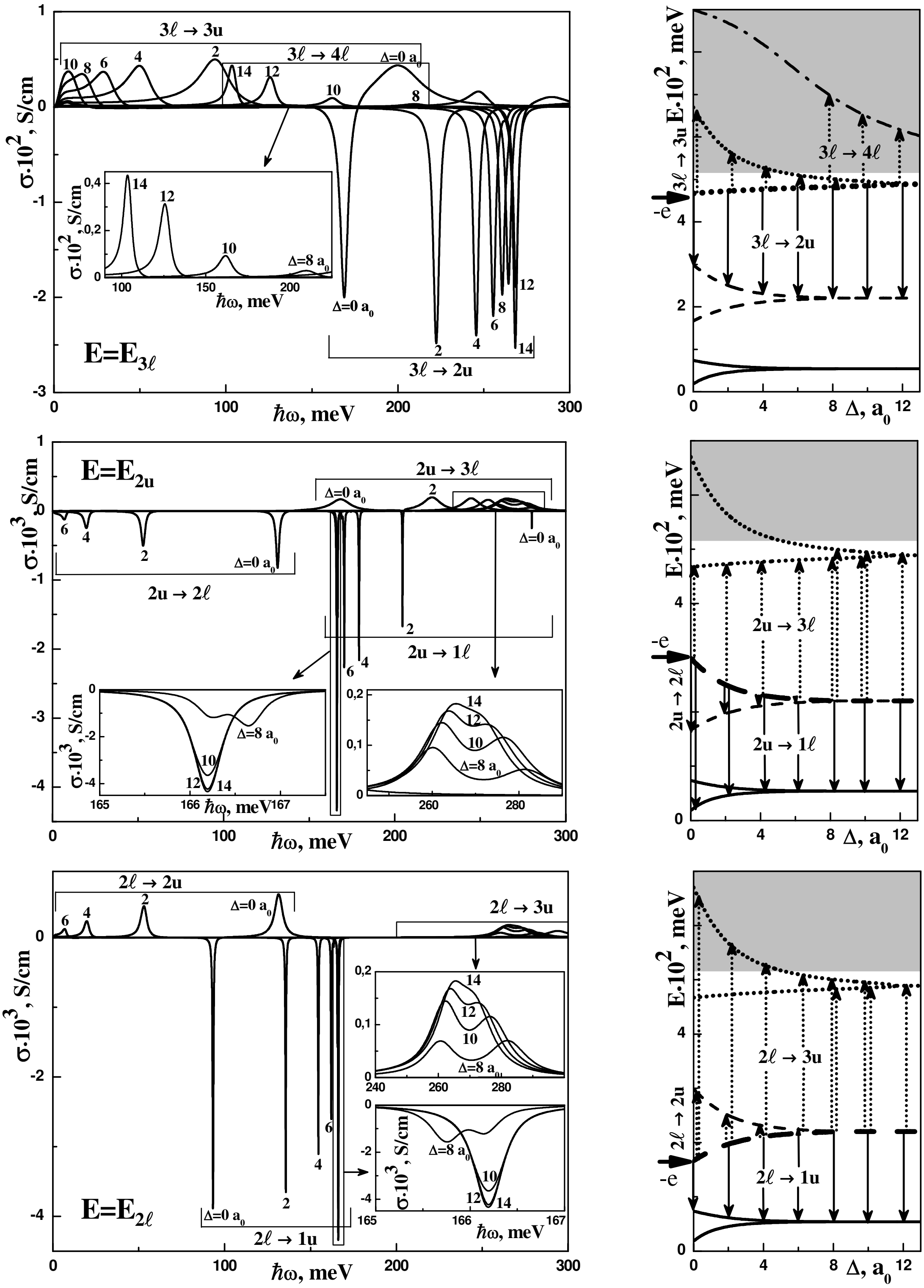

Fig. 4. Dependences of the conductivity σ on the field energy $\hbar\omega$ (at the energies $E = E_{2\ell}$, E_{2u}, and $E_{3\ell}$ and the concentration $n_0 = 10^{16}$ cm^{-3} of incident electrons) and the resonance energies E on the interior barrier thickness Δ in the rectangular potential model at $b = 15a_0$ and $\Delta_1 = 4a_0$

out in the framework of the rectangular potential model for the electron concentration $n_0 = 10^{16}$ cm^{-3} and the TBRTS dimensions $b = 15a_0$ and $\Delta_1 = 4a_0$. One can see that the basic properties of the conductivity and the origin of their emergence are the same as in the case analyzed earlier. However, some new aspects should be emphasized. They are as follows.

In the case where $E = E_{2\ell}$, besides the transitions $2\ell \rightarrow 2u$ and $2\ell \rightarrow 1u$ which take place being accompanied by radiation absorption and emission, respectively, another positive peak of $\sigma(\omega)$ is observed in the high-frequency region, which corresponds to the transition $2\ell \rightarrow 3u$. As Δ increases, the positive low-energy peak intensity in $\sigma(\omega)$ gradually decreases from its maximum value to zero, whereas the high-energy peak intensity, on the contrary, increases from zero and saturates at its maximum.

The case where $E = E_{2u}$ is similar to the previous one. Here, the positive part of $\sigma(\omega)$ is formed by a single transition, $2u \rightarrow 3\ell$, whereas the negative one by two transitions, $2u \rightarrow 2\ell$ and $2u \rightarrow 1\ell$.

In the case $E = E_{3\ell}$, the behavior of $\sigma(\omega)$ in the transitions $3\ell \rightarrow 3u$ and $3\ell \rightarrow 2u$ is analogous to the previous ones. The appearance of an intensive $3\ell \rightarrow 4\ell$ transition, which is accompanied by the absorption of an electromagnetic wave, can be explained as follows. This transition is formally classified as a forbidden one. However, the corresponding QSES with the energy $E_{4\ell}$ is located in the overbarrier energy range, where the properties of quasistationary states are substantially different from those of subbarrier states.

4. Conclusions

The developed theory of conductivity in a symmetric TBRTS shows that the δ-barrier model reproduces all main properties of this parameter but shifts the whole picture, as compared with the model of rectangular potentials, toward the high-frequency range. The maximal and minimal values are reduced by a factor of several tens. It is shown that the negative and positive conductivities are associated with the quantum transitions between electron levels of size quantization which are accompanied by the emission and the absorption, respectively, of an electromagnetic wave. In the ranges of frequencies which are of the order of widths of those QSES, into which transitions occur, the TBRTS can operate as either a laser emitter (the negative conductivity) or a sensor (the positive conductivity). The analysis of properties of $\sigma(\omega)$ in both potential models shows that, when the interior barrier thickness falls in the "pre-collapse" region, positive and negative peaks of conductivity are formed by quantum transitions between neighbor QSESs: $n\ell \leftrightarrow nu$ and $n\ell \leftrightarrow (n \pm 1)u$ (up and down, respectively, on the energy scale). Transitions $n\ell(u) \rightarrow n'\ell(u)$ are forbidden, i.e. they do not manifest themselves in the frequency dependence $\sigma(\omega)$. The intensities of the transitions $n\ell \leftrightarrow n'u$ drastically decrease, when the difference $|n - n'|$ and the resonance energy of a monoenergetic electron beam that bombards the RTS increase.

In the "post-collapse" interval of interior barrier thicknesses, the degenerate spectrum of symmetric TBRTS behaves itself like a spectrum of asymmetric two-barrier RTS with a thin left barrier and a wide right one. For such a system, the quantum transitions $n \rightarrow n \pm 1$ manifest themselves in the dependence σ versus ω (see insets in Fig. 4). Although the transitions in such RTSs can be rather intense (Fig. 4), the transmission factor of the system drastically decreases ($D \rightarrow 0$) due to the existence of a too powerful interior barrier. The electron beam is almost completely reflected from the wide interior barrier, being directed oppositely to its initial direction of motion. It is clear that symmetric TBRTSs with an interior barrier possessing the "post-collapse" thickness cannot serve as a base elements for quantum cascade lasers, irrespective of which mode they operate in: classical (phonon-assisted transitions) or ballistic. All known experimentally realized quantum cascade lasers, which are based on TBRTS [16, 16], are so designed that the interior barrier should always be narrower than any other external one.

1. J. Faist, F. Capasso, D.L. Sivco, C. Sirtori, A.L. Hutchinson, and A.Y. Cho, Science **264**, 553 (1994).
2. J. Faist, F. Capasso, and C. Sirtori, Appl. Phys. Lett. **66**, 538 (1995).
3. V.F. Elesin, Zh. Eksp. Teor. Fiz. **116**, 704 (1999).
4. E.I. Golant and A.B. Pashkovskii, Pis'ma Zh. Eksp. Teor. Fiz. **67**, 372 (1998).
5. M.V. Tkach and Yu.O. Seti, Ukr. Fiz. Zh. **54**, 614 (2009).
6. N.V. Tkach and Yu.A. Seti, Fiz. Tekh. Poluprovodn. **43**, 1346 (2009).
7. V.F. Elesin, Zh. Eksp. Teor. Fiz. **126**, 131 (2005).
8. V.F. Elesin and I.Yu. Kateev, Fiz. Tekh. Poluprovodn. **42**, 586 (2008).
9. V.F. Elesin, I.Yu. Kateev, and M.A. Remnev, Fiz. Tekh. Poluprovodn. **43**, 269 (2009).

10. A.B. Pashkovskii, Pis'ma Zh. Eksp. Teor. Fiz. **82**, 228 (2005).
11. E.A.Gelvich, E.I. Golant, and A.B. Pashkovskii, Pis'ma Zh. Eksp. Teor. Fiz. **32**, 13 (2006).
12. A.B. Pashkovskii, Pis'ma Zh. Eksp. Teor. Fiz. **89**, 32 (2009).
13. A.A. Gorbatsevich, M.N. Zhuravlev, and V.V. Kapaev, Zh. Eksp. Teor. Fiz. **134**, 338 (2008).
14. N.V. Tkach and Yu.A. Seti, Fiz. Nizk. Temp. **35**, 710 (2009).
15. C. Gmachl, F. Capasso, D.L. Sivco, and A.Y. Cho, Rep. Prog. Phys. **64**, 1533 (2001).
16. A.K.M. Newaz, W. Song, E.E. Mendez, Y. Lin, and J. Nitta, Phys.Rev. B **71**, 195303 (2005).

Received 18.12.09.
Translated from Ukrainian by O.I. Voitenko

КВАЗІСТАЦІОНАРНІ СТАНИ ЕЛЕКТРОНА І ПРОВІДНІСТЬ СИМЕТРИЧНОЇ ТРИБАР'ЄРНОЇ РЕЗОНАНСНО-ТУНЕЛЬНОЇ СТРУКТУРИ

М.В. Ткач, Ю.О. Сеті

Р е з ю м е

У моделях прямокутних і δ-подібних потенціальних бар'єрів симетричної трибар'єрної резонансно-тунельної структури (ТБРТС) досліджено еволюцію спектральних параметрів (резонансних енергій і ширин) квазістаціонарних станів електрона залежно від геометричних параметрів наносистеми. У наближенні малої величини напруженості електричного поля знайдено провідність симетричної ТБРТС. Встановлено, що в моделі δ-подібних потенціальних бар'єрів, внаслідок ігнорування різниці ефективних мас електрона у ямах та у бар'єрах, максимальні значення провідності виявляються заниженими у десятки разів порівняно з більш реалістичною моделлю прямокутних потенціалів.